

AFFINE-INVARIANT ELLIPTICAL STATE ESTIMATION FOR ROBUST EXTENDED OBJECT TRACKING

In Ho Lee[1]

[1]Korea Institute of Industrial Technology

Abstract

Extended object tracking (EOT) has emerged as a critical challenge in modern surveillance and autonomous systems, where high-resolution sensors yield multiple measurements per target in a single scan. This task necessitates the simultaneous estimation of an object's spatial extent and kinematic states by systematically assimilating distributed detections. In practical scenarios, however, sensor visibility constraints often restrict measurements to partial contours rather than the full object geometry, posing a significant hurdle for accurate state estimation. This paper proposes a robust EOT algorithm that addresses these challenges by extracting elliptical features—including size, orientation, and noise characteristics—in an affine-invariant manner from incomplete measurement sets. By formulating the ellipse-fitting problem through an algebraic solution, the proposed method effectively reconstructs the target's morphology even under severe self-occlusion. The tracking framework is established as a Bayesian inference problem, utilizing a standard Kalman filter as a recursive estimator to ensure both computational efficiency and numerical robustness. The performance of the proposed approach is validated through comparative analyses with state-of-the-art algorithms using both synthetic trajectories and real-world LiDAR datasets. The results demonstrate that the proposed method significantly outperforms existing benchmarks in estimation accuracy and real-time processing, particularly in scenarios characterized by partial observability and complex maneuvers.

Keywords: extended object tracking, Kalman filtering, elliptical target model, affine transformation.

1. Introduction

Extended Object Tracking (EOT) has become a pivotal challenge in modern surveillance and autonomous systems. Unlike conventional point target tracking, which simplifies an object to a single measurement point per time step, EOT accounts for the non-negligible spatial extent of targets such as vehicles, vessels, and aircraft, which inherently generate multiple measurements. Consequently, EOT frameworks aim to concurrently estimate both kinematic states and spatial morphology (i.e., shape) from sensor data, thereby enabling high-fidelity tracking and robust trajectory forecasting [1, 2, 3]. Driven by the recent proliferation of high-resolution far-field sensors [4], the significance of EOT is rapidly expanding across various industrial domains. For instance, LiDAR or radar systems integrated into autonomous platforms often receive multiple reflections from diverse points along an object's contour within a single scan, necessitating advanced EOT techniques to process these complex measurement sets. In contrast to the point-mass tracking paradigm, the EOT framework involves the processing of numerous measurements whose spatial distribution depends not only on the object's kinematic states but also on its geometric configuration. This dependency introduces significant modeling challenges, as it requires sophisticated stochastic processes to accurately represent the measurement generation associated with extended targets. To address these complexities, extensive research has been conducted to develop robust EOT algorithms. A predominant strategy in these efforts is to model the target geometry using fundamental primitives, such as ellipses [5, 6],

rectangles [7], or star-convex shapes [8]. In scenarios characterized by diverse object classes and high-density measurements, such geometric simplifications are highly effective, as they ensure computational tractability while maintaining sufficient descriptive power for tracking tasks.

This paper investigates target-tracking methodologies employing elliptical models, with a specific focus on the inherent characteristics of sensor measurement data. The Random Matrix Model (RMM) has established itself as a robust framework, offering an approximate Bayesian solution by modeling elliptical extensions via the inverse Wishart distribution, while representing kinematic states through a Gaussian distribution [9, 10, 11]. Alternatively, Extended Kalman Filter (EKF)-based approaches [6, 12] utilize explicit ellipse parameterization, enabling individual extension parameters to maintain distinct uncertainty representations. Although effective in sparse measurement scenarios, the sequential update mechanism of EKF-based methods can become computationally prohibitive in dense measurement environments. Recent batch-based adaptations of MEM-EKF* mitigate the computational burden associated with sequential updates [13], yet still rely on full-surface measurement assumptions. To mitigate this, alternative strategies leverage principal components for efficient parameter updates. For instance, a method involving the estimation of semi-axes through the eigenvalue decomposition of the dispersion (or scatter) matrix was introduced in [14]. Similarly, the Principal Axes Kalman Filter (PAKF) operates on the assumption of a Gaussian spatial distribution of measurements, extracting elliptical parameters directly from a pre-processed dispersion matrix [15]. Despite their respective merits, a critical underlying assumption across most of these algorithms is that measurements are ideally and uniformly distributed over the object's surface.

Crucially, the acquisition of measurement data is inherently constrained by the sensor-to-object geometry; sensors only receive reflections from surfaces oriented toward them. This phenomenon, governed by the non-penetrative nature of sensor beams, results in partial observations—often referred to as self-occlusion—preventing the direct capture of an object's complete morphology from raw measurements alone. Consequently, assuming an appropriate geometric prior is essential to enhance the joint estimation of both the object's spatial extent and its kinematic state. In this paper, we propose a novel ellipse-generation framework that characterizes the object's extent based on observed contour fragments. Unlike conventional bounding-box approaches, the proposed method approximates arbitrary morphologies as elliptical representations, enabling the robust inference of global dimensions and orientation (rotational pose) even from fragmentary observations. Given the prevalence of elliptical geometries in both natural and man-made environments, our approach offers broad applicability across various domains necessitating the estimation of stochastic object shapes.

This study presents a robust elliptical state estimation algorithm specifically designed for EOT under partial contour observations. The framework integrates the sensor-to-object geometry to address the inherent limitations of incomplete measurement data. Initially, an augmented state vector is constructed to encapsulate both kinematic states and geometric parameters, ensuring a high-fidelity representation of the extended object. Subsequently, the partial outlines of the target are delineated based on the intersecting geometry between the sensor beam and the object boundary, accounting for the relative angular and radial constraints. To achieve invariance against sensor noise and fluctuations in object scale or orientation, an affine transformation is applied to the extracted features. The elliptical fitting problem is then rigorously solved using a least-squares approach via Singular Value Decomposition (SVD). Finally, the proposed measurement model is integrated into a recursive Bayesian inference framework, utilizing a Kalman filter to propagate and update the posterior probability density functions.

The main contributions of this paper are:

1. This paper addresses extended object tracking under boundary-only LiDAR measurements, explicitly considering the sensor–object geometry that restricts observations to sensor-facing contour regions rather than the full object surface.

2. An affine-invariant coordinate normalization framework is proposed to robustly extract elliptical extent parameters (semi-axes and orientation) from incomplete and anisotropically distributed boundary measurements.

3. The proposed algebraic ellipse fitting solution is integrated into a Kalman filter–based Bayesian

estimation framework, enabling efficient joint estimation of kinematic and extent states.

4. Through simulations and real LiDAR data experiments, the method demonstrates improved extent estimation accuracy in scenarios where measurements originate only from visible object contours, a setting that challenges conventional surface-based extended object trackers.

The remainder of this paper is organized as follows: Section II defines the problem formulation and the Bayesian filtering framework. Section III details the proposed ellipse-generation methodology. Experimental validations and performance evaluations using both synthetic and real-world datasets are discussed in Section IV, followed by concluding remarks in Section V.

2. Bayesian Filter

For the sake of analytical simplicity, this study assumes that the extended target operates within a two-dimensional (2-D) plane, with its geometry represented by a projected 2-D contour. Consider a scenario where a single object generates a set of multiple measurements, denoted as $\mathbf{Y}_k = \{\mathbf{y}_k^i\}_{i=1}^n$, within a individual sensor scan or frame. Unlike conventional point-target tracking paradigms that focus exclusively on estimating kinematic states (e.g., position and velocity), EOT necessitates a more comprehensive framework. Such a framework must define an augmented state vector that encapsulates both the object's pose and its spatial morphology, governed by a dynamic model that characterizes the temporal evolution of these states. Fundamentally, the objective of EOT is the joint estimation of the target's trajectory and its geometric extent.

2.1 Dynamic Model for EOT

The dynamic model can be characterized in general terms as follows:

$$\mathbf{X}_{k+1} = \mathbf{f}(\mathbf{X}_k, \mathbf{w}_k) \tag{1}$$

where $\mathbf{X}_k$ denotes the object state vector at time step k, $\mathbf{w}_k \in \mathbb{R}^m$ represents the zero-mean additive white Gaussian noise with covariance $\mathbf{Q}_k \in \mathbb{R}^{m\times m}$, and $\mathbf{f}(\cdot)$ is the state transition function. We define the state of the extended object as a composite vector comprising its kinematic state, $\mathbf{x}_k^c = [\mathbf{m}_k, \dot{\mathbf{m}}_k]^T$—representing the Cartesian center position and its velocity—and its elliptically approximated extent state, $\mathbf{x}_k^s = [a_k, b_k, \theta_k]^T$, consistent with the formulations in [16, 17, 6]. Assuming an approximate decoupling between the centroid kinematics and the object's spatial extension, along with their respective independent dynamic models, the standard Kalman filter prediction framework can be directly applied. Analogous to the decomposition of the state vector, the transition function $\mathbf{f}$ can be partitioned into two distinct components to separately characterize the temporal evolution of the pose and shape states. This decomposition is formulated as follows:

$$\begin{bmatrix}\mathbf{x}_{k+1}^c \\ \mathbf{x}_{k+1}^s\end{bmatrix} = \begin{bmatrix}\mathbf{f}^c(\mathbf{x}_k^c, \mathbf{w}_k^c) \\ \mathbf{f}^s(\mathbf{x}_k^s, \mathbf{w}_k^s)\end{bmatrix} \tag{2}$$

In this formulation, $\mathbf{w}_k^c$ and $\mathbf{w}_k^s$ are the constituent noise vectors of $\mathbf{w}_k$, characterizing the process uncertainties of the kinematic and shape dynamics with associated covariances $\mathbf{Q}_k^c$ and $\mathbf{Q}_k^s$, respectively. The specific functional form of $\mathbf{f}_k^c$ is dictated by the definition of the kinematic state $\mathbf{x}_k^c$ and the adopted motion model. Furthermore, this study assumes time-invariant geometries, which implies that the shape transition $\mathbf{f}_k^s$ is modeled as an identity mapping, such that $\mathbf{x}_{k+1}^s = \mathbf{x}_k^s + \mathbf{w}_k^s$.

2.2 Measurement Source and Information

In existing literature, it is common to assume that measurements follow a Gaussian distribution, with the standard deviation proportional to the object's spatial extent. However, it is imperative to address the limitations of estimating the state of an extended object based solely on this Gaussian assumption. As illustrated in Fig. 1, the spatial relationship between the sensor and the measurement sources Z_k reveals that the actual data generation process is far more complex. Consequently, measurements do not conform to a simplistic analytical distribution. This inherent complexity arises because measurements are generated by the intersection of sensor beams with the object's contours, a process inherently corrupted by stochastic noise. Thus, the resulting measurement distribution

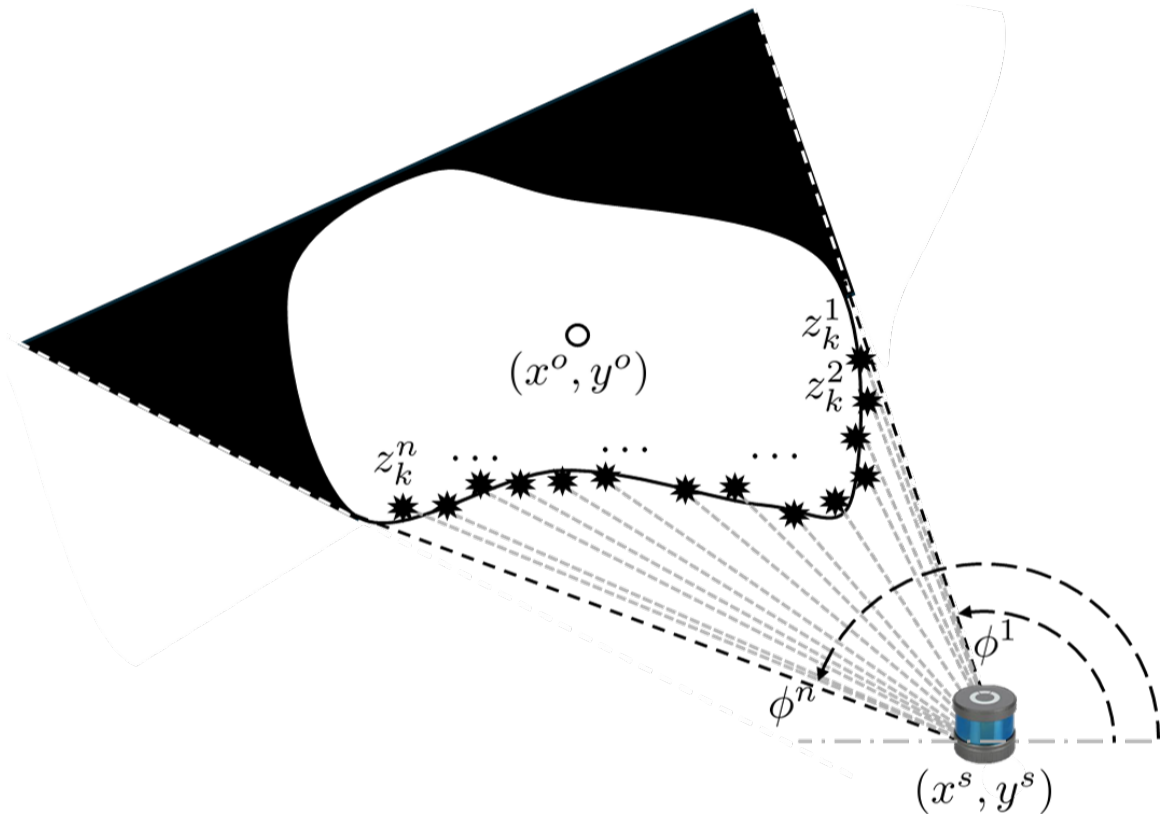


Figure 1 – A set of measurement sources Z_k obtained within a scan at time k that take into account the sensor-object geometry.

cannot be directly characterized by standard probability density functions. Furthermore, given the sensor-object geometry, inferring the true elliptical morphology from fragmentary contour segments remains a significant challenge. Since available measurements often fail to encapsulate the complete geometric profile of the target, relying exclusively on these data points may lead to insufficient penalization of improbable state representations during the measurement update. This can result in the misallocation of posterior probability mass to erroneous states, introducing biases and inflating uncertainty. Ultimately, such inaccuracies lead to a non-negligible degradation in overall tracking performance.

Drawing on the framework proposed in [8], the measurements captured from the object's surface can be characterized by a scaling parameter. Consequently, any measurement source residing on the boundary of an elliptical extended object can be formulated as:

$$Z_k = \mathbf{m}_k + \begin{bmatrix} cos(\theta_k) & -sin(\theta_k) \\ sin(\theta_k) & cos(\theta_k) \end{bmatrix} \begin{bmatrix} a_k & 0 \\ 0 & b_k \end{bmatrix} \begin{bmatrix} cos(\phi^i) \\ sin(\phi^i) \end{bmatrix} \tag{3}$$

In this context, $\mathbf{m}_k$ denotes the centroid of the extended object, while θ_k, a_k, and b_k represent its orientation and semi-axes lengths, respectively. Let ϕ^i denote the parametric angle of the intersection point on the ellipse. The sensor's field of view (FoV), or opening angle, is bounded by the minimum and maximum angles, x_1 and x_n. The angular resolution is determined by the step size y_1, defined as the angular increment between consecutive measurements (i.e., $y_1 = x_i - x_j$). As illustrated in Fig. 1, the object's angular extent is succinctly characterized by the extrema of the angles subtended at the sensor within its operational range. Typically, these boundary angles can be efficiently extracted from raw measurement data through optimized post-processing techniques. Let $\mathbf{p}^s = [x^s, y^s]^T$ be the sensor position and Z_k denote the target geometry to be estimated. The configuration is subsequently approximated by a discrete sequence of n points corresponding to the state vector. Consequently, the angular coordinate (or phase angle) can be formulated as follows:

$$y = tan(\phi^i)(x - x^s) + y^s \tag{4}$$

To find the intersections on the object contour, (4) is inserted in the equation of an ellipse $x^2/a^2 + y^2/b^2 = 1$, we can easily get

$$\left(\frac{b^2 + a^2 tan^2(\phi^i)}{a^2 b^2}\right) x^2 + 2\left(\frac{tan(\phi^i) y^s - tan^2(\phi^i) x^s}{b^2}\right) x + \left(\frac{y^s - tan(\phi^i) x^s}{b}\right)^2 - 1 = 0 \tag{5}$$

Equation (5) yields a closed-form solution via a quadratic polynomial. To distinguish the sensor-facing boundary of the object from the two algebraic solutions, we identify the point that minimizes the expected Euclidean distance to the sensor, denoted as $[x_m, y_m]^T$. By integrating the sensor's spatial coordinates, the measurement source located on the contour of the extended target can be explicitly formulated by substituting the proposed approach into (3).

$$Z_k = m_k + \begin{bmatrix} cos(\theta_k) & -sin(\theta_k) \\ sin(\theta_k) & cos(\theta_k) \end{bmatrix} \begin{bmatrix} x_m \\ y_m \end{bmatrix} \tag{6}$$

At each discrete time step, the extended object yields a stochastic number of independent 2-D detections. Each constituent measurement within the set $\mathbf{Y}_k$ is assumed to emanate from a specific latent measurement source Z_k located on the object's boundary. These observations are inherently corrupted by zero-mean additive white Gaussian noise (AWGN), denoted by $\mathbf{v}$, with a corresponding covariance matrix $\mathbf{C}^{\mathbf{v}}$.

$$\mathbf{y}_k^i = Z_k + \mathbf{v}_k^i \tag{7}$$

In the following the section, details for deriving measurement model are presented.

3. Elliptical based approach to EOT

Given the inherent geometric constraints between the sensor and the target, it is evident that reconstructing the complete spatial profile of an extended object from fragmentary contour observations is an inherently ill-posed problem. To address this challenge, employing an elliptical prior serves as an effective strategy for robustly estimating the object's morphology in unobserved regions.

3.1 Affine Invariant Coordinate Transformation

It is essential to acknowledge that measurement characteristics of the same object can fluctuate significantly due to variations in sensor configurations and the intrinsic properties of the target. To ensure consistent tracking performance, it is imperative to employ a target descriptor that remains invariant to such geometric transformations. In this context, affine invariants are frequently utilized to maintain the structural integrity of the measurements under affine transformations. This property is crucial for accurately analyzing the morphology and underlying structure of the observed data. Particularly in applications involving elliptical models, affine invariants provide robust stability against variations in scale, orientation, and noise-induced distortions. Consequently, this invariance facilitates reliable state estimation across diverse and challenging sensing environments.

Under noise-free conditions, the object's geometry can be theoretically inferred directly from sensor observations. In practice, however, the presence of stochastic noise and the specific sensor-target geometry markedly influence the estimation of the spatial extent, with the impact varying significantly across different measurement locations. Furthermore, the measurement representations characterized in (7) do not inherently exhibit invariance to affine transformations—a property highly desirable for robust EOT. To address this limitation, we propose a methodology to transform the measurement coordinate system. To achieve a measurement representation that remains invariant under affine transformations, the original coordinate system must be reconfigured. Building upon (7), we aim to identify a linear transformation matrix $\mathbf{L} \in \mathbb{R}^{2\times 2}$ and a translation vector $\mathbf{t} \in \mathbb{R}^2$ such that the resulting vectors satisfy the following invariant properties:

$$\tilde{\mathbf{y}}_k^i = \mathbf{L}(\mathbf{y}_k^i - \mathbf{t}_k) \tag{8}$$

The objective is to ensure that the transformed vectors exhibit a zero mean and an identity covariance matrix $\mathbf{I}$. Denoting the transformed measurement set as $\tilde{\mathbf{Y}}_k = [\tilde{\mathbf{y}}^1, \cdots, \tilde{\mathbf{y}}^n]$, this condition necessitates that $\tilde{\mathbf{Y}}_k \tilde{\mathbf{Y}}_k^T = \mathbf{I}$, effectively whitening the measurement distribution. To perform the centering operation on $\mathbf{Y}$, it is necessary to define the following parameters:

$$\mathbf{t}_k = \frac{1}{n} \sum_{i=1}^{n} \mathbf{y}_k^i \tag{9}$$

Let $\overline{\mathbf{Y}}_k = [\mathbf{y}^1 - \mathbf{t}_k, \cdots, \mathbf{y}^n - \mathbf{t}_k]$ denote the ensemble of centered measurement vectors. The eigenvalue decomposition (EVD) of the resulting scatter matrix, $\overline{\mathbf{Y}}_k \overline{\mathbf{Y}}_k^T$, is then expressed as:

$$\overline{\mathbf{Y}}_k \overline{\mathbf{Y}}_k^T = \mathbf{U} \Sigma \mathbf{U}^T \tag{10}$$

By considering

$$\mathbf{L} = \Sigma^{-1/2} \mathbf{U}^T \tag{11}$$

we obtain the desired result.

3.2 Ellipse Constrained Estimation

To facilitate extended object tracking (EOT), established methodologies such as RMM [9], MEM-EKF [6], and variational Bayesian inference [18] employ recursive Bayesian techniques to derive posterior approximations through iterative measurement updates. However, these frameworks often become computationally prohibitive as the complexity scales with the increasing volume of measurements or the number of targets. An alternative strategy involves the direct estimation of elliptical extent parameters from sensor data. Conventionally, these parameters are updated by decomposing the measurement scatter matrix into its principal components, predicated on the assumption that measurements are uniformly sampled from a random surface and follow a Gaussian distribution. In practice, however, this assumption is frequently violated because physical sensors primarily capture the target's contour with high intensity. To address this discrepancy, we propose a robust method to estimate elliptical extent parameters from observed contour segments. The core of the proposed algorithm lies in effectively addressing the well-established challenge of fitting ellipses to point cloud data.

A conic section is analytically defined as the locus of points $\tilde{\mathbf{y}} = [\tilde{x}, \tilde{y}]^T$ in the Cartesian coordinate system that satisfy a general quadratic equation.

$$a_{11}\tilde{x}^2 + 2a_{12}\tilde{x}\tilde{y} + a_{22}\tilde{y}^2 + b_1\tilde{x} + b_2\tilde{y} + c = 0 \tag{12}$$

where $a_{11}, a_{12}, a_{22}, b_1, b_2$, and c are real-valued coefficients satisfying the condition $a_{11}^2 + a_{12}^2 + a_{22}^2 > 0$. By utilizing the coordinate vector $\tilde{\mathbf{y}}$, (12) can be equivalently expressed in the following quadratic form:

$$\tilde{\mathbf{y}}^T \begin{bmatrix} a_{11} & a_{12} \\ a_{12} & a_{22} \end{bmatrix} \tilde{\mathbf{y}} + \begin{bmatrix} b_1 & b_2 \end{bmatrix} \tilde{\mathbf{y}} + c = 0 \tag{13}$$

By defining $\mathbf{A} = \begin{bmatrix} a_{11} & a_{12} \\ a_{12} & a_{22} \end{bmatrix}$, $\mathbf{B} = \begin{bmatrix} b_1 & b_2 \end{bmatrix}$, and $C = c$, (13) takes the quadratic form $\tilde{\mathbf{y}}^T \mathbf{A} \tilde{\mathbf{y}} + \mathbf{B}\tilde{\mathbf{y}} + C = 0$. Consequently, an ellipse E can be uniquely characterized by the triplet $(\mathbf{A}, \mathbf{B}, C)$ through an implicit equation of the following form:

$$E = \left\{ \tilde{\mathbf{y}} \in \mathbb{R}^2 | \tilde{\mathbf{y}}^T A \tilde{\mathbf{y}} + B\tilde{\mathbf{y}} + c = 0 \right\} \tag{14}$$

In this formulation, $\mathbf{A} \in \mathbb{R}^{2\times 2}$ is defined as a symmetric positive definite (SPD) matrix, while $\mathbf{B} \in \mathbb{R}^2$ and $C \in \mathbb{R}$ denote a vector and a scalar, respectively. These variables constitute the model parameters to be estimated, with the ultimate objective of selecting optimal values that maximize the fidelity of the model to the empirical measurement data.

In the presence of measurement noise, it is impossible for all empirical data points to strictly satisfy (14). Consequently, it is pragmatic to adopt an optimization framework that minimizes the residual error with respect to a specific norm. The algebraic fitting approach focuses on minimizing the following residual objective function:

$$G(A,B,C) = \sum_{i=1}^{n} ((\tilde{\mathbf{y}}^i)^T A \tilde{\mathbf{y}}^i + B\tilde{\mathbf{y}}^i + c)^2 \tag{15}$$

Consistent with the methodology delineated in [19], we impose the trace constraint $Tr(\mathbf{A}) = 1$. This specific formulation offers the distinct advantage of introducing a convex constraint, thereby streamlining the development of efficient numerical optimization algorithms. Consequently, the global optimization problem is formulated as follows:

$$\underset{(\{A,B,C\}\in\mathscr{M})}{min} \; G(A,B,C) \quad s.t. \;\; Tr(A) = 1 \tag{16}$$

Various methodologies have been explored in the literature to solve the optimization problem (16), as documented in [20, 21]. In this study, we propose an alternative approach as follows. We define a coefficient vector $\mathbf{q} = [a_{11}, \sqrt{2}a_{12}, a_{22}, b_1, b_2, c]^T$ and a corresponding feature vector of quadratic monomials derived from the measurements, $\mathbf{d}^i = [(\tilde{x}^i)^2, \sqrt{2}\tilde{x}^i\tilde{y}^i, (\tilde{y}^i)^2, \tilde{x}^i, \tilde{y}^i, 1]^T$. By employing these vector representations, the optimization problem (16) can be reformulated as:

$$\underset{\mathbf{q}}{min}\, \mathbf{q}^T DD^T \mathbf{q} = \left\|\mathbf{q}^T D\right\|^2 \quad s.t. \;\; Tr(\mathscr{S}(q)) = 1 \tag{17}$$

where $\mathbf{D} = [\mathbf{d}^1, \ldots, \mathbf{d}^n]^T$ represents the design matrix, and $\mathscr{S}(\cdot)$ denotes the linear operator designed to extract the leading 2×2 sub-matrix from the vectorized parameters. A computationally efficient and robust approach to solving the ellipse fitting problem involves utilizing Singular Value Decomposition (SVD) to obtain the total least squares solution. Under the unit-norm constraint, the optimal parameter vector $\hat{\mathbf{q}}$ is identified as the right singular vector of $\mathbf{D}$ corresponding to its minimum singular value (or equivalently, the eigenvector of $\mathbf{D}^T\mathbf{D}$ associated with its smallest eigenvalue).
To ensure algorithmic invariance, the coordinate system was reconfigured through a normalization process. Subsequent processing of the point cloud was conducted using a normalized centroid characterized by an identity covariance matrix, as delineated in (8). Once the estimated coefficients $\hat{\mathbf{q}}$ are obtained within this modified system, they must be mapped back to the original coordinate frame to retrieve the physical parameters of the extended object. By mapping the estimated coefficient vector $\hat{\mathbf{q}}$ back into its matrix-vector representation, the resulting triplet $(\mathbf{A}', \mathbf{B}', C')$ in the original coordinate frame is obtained as follows:

$$A' = \begin{bmatrix} \hat{q}_1 & \frac{\hat{q}_2}{\sqrt{2}} \\ \frac{\hat{q}_2}{\sqrt{2}} & \hat{q}_3 \end{bmatrix}, B' = \begin{bmatrix} \hat{q}_4 & \hat{q}_5 \end{bmatrix}, \text{ and } C' = \hat{q}_6 \tag{18}$$

The triplet minimizer $(\mathbf{A}, \mathbf{B}, C)$ exhibits equivariance (or covariance) under the translation and rotation of the measurement ensemble $\mathbf{Y}$. Specifically, let $\hat{E}'$ denote the ellipse obtained by solving the optimization problem (14) using the normalized coordinates $\tilde{\mathbf{Y}}$ defined in (8). If $\hat{E}$ represents the optimal elliptical solution in the original coordinate frame, then the geometric relationship is given by $\hat{E} = \mathbf{L}^{-1}\hat{E}' + \mathbf{t}$. Accordingly, the triplet parameters in the original space are recovered as:

$$\begin{aligned} A &= L^T A' L \\ B &= -2A\mathbf{t} + B'L \\ C &= \mathbf{t}^T A\mathbf{t} - B'L\mathbf{t} + C' \end{aligned} \tag{19}$$

3.3 Elliptical Extended Object Tracking Problem

By utilizing the recovered general-form coefficients, the canonical parameters—specifically the estimated centroid (x_c, y_c), the semi-axes lengths (a, b), and the orientation angle θ—can be extracted through the following analytical geometry relationships:

$$\hat{m} = \begin{bmatrix} \hat{x}^c \\ \hat{y}^c \end{bmatrix} = \left[\frac{a_{22}b_1 - a_{12}b_2}{2(a_{12}^2 - a_{11}a_{22})}, \frac{a_{11}b_2 - a_{12}b_1}{2(a_{12}^2 - a_{11}a_{22})} \right]^T \tag{20}$$

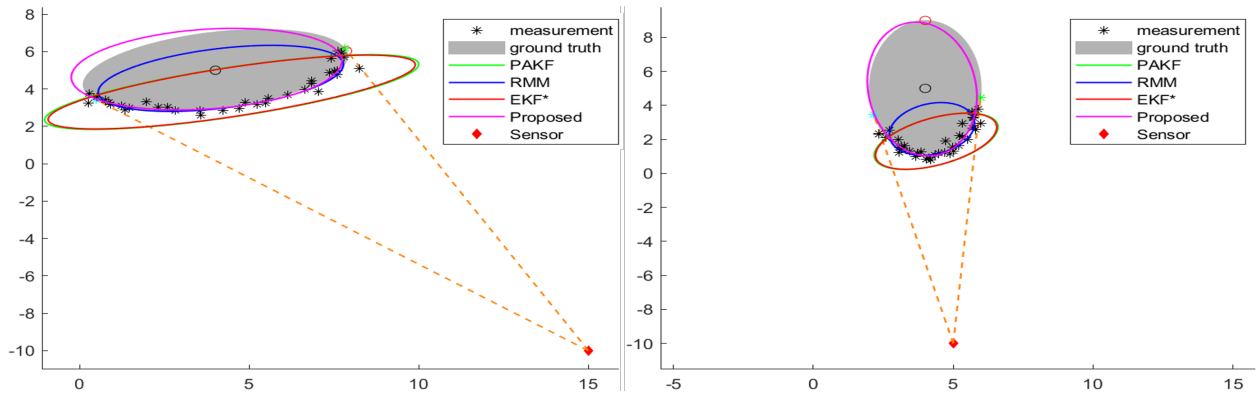


Figure 2 – Simulation of stationary object

$$\begin{bmatrix}\hat{a}\\ \hat{b}\end{bmatrix} = -\frac{\sqrt{2(a_{11}b_2^2+a_{22}b_1^2-2a_{12}b_1b_2+4(a_{12}^2-a_{11}a_{22})c)}}{4(a_{12}^2-a_{11}a_{22})} \times \begin{bmatrix}\sqrt{((a_{11}+a_{22})+\sqrt{(a_{11}-a_{22})^2+4a_{12}^2})}\\ \sqrt{((a_{11}+a_{22})-\sqrt{(a_{11}-a_{22})^2+4a_{12}^2})}\end{bmatrix} \tag{21}$$

$$\hat{\theta} = \frac{1}{2}\arctan\left(\frac{a_{11}-a_{22}}{2a_{12}}\right) \tag{22}$$

The measurement model at time k, encompassing both kinematic and extent states, is formulated through a nonlinear observation function $\mathbf{h}(\cdot)$ as follows:

$$\hat{\mathbf{y}}_k^c = \hat{m}_k + v_k^c = H^c\mathbf{x}_k^c + v_k^c \tag{23}$$

$$\hat{\mathbf{y}}_k^s = \hat{\mathbf{x}}_k^s + v_k^s \tag{24}$$

Let $\mathbf{Y}_k$ denote the set of measurements at time k. The problem of tracking extended objects within an elliptical framework is formulated as a recursive state estimation task. In this context, the primary objective is to derive the posterior probability density function (PDF) of the unknown state vector X_k, conditioned on the cumulative measurements.

$$p(\mathbf{X}_k|\mathbf{Y}_1,\cdots,\mathbf{Y}_k) \tag{25}$$

The state estimate $\hat{\mathbf{X}}_k$ is determined as the mean of the posterior distribution. The computation, as formulated in (25), is performed recursively by leveraging the framework of Bayes' theorem. Within this architecture, the distribution is propagated using the dynamic model defined in (2) and subsequently updated via the measurement models provided in (23) and (24). In this study, a standard Kalman filter is employed as the recursive state estimator to achieve computational efficiency.

4. Experimental results

We evaluate the performance of the proposed algorithm using both synthetic and empirical datasets, benchmarking it against established methods such as RMM [10], EKF [6], and PAKF [15]. Initially, the accuracy of the proposed elliptical moment approximation is validated through numerical simulations. Subsequently, the advantages of the proposed tracker are demonstrated by comparing its performance with existing methodologies under simple extended dynamics, where target trajectories are generated in consideration of the inherent sensor-target geometry. Finally, the efficacy and robustness of the proposed approach are further validated using real-world LiDAR data. To rigorously quantify the estimation accuracy, the Gaussian Wasserstein (GW) distance between the estimated and ground-truth ellipses is adopted as the primary performance metric.

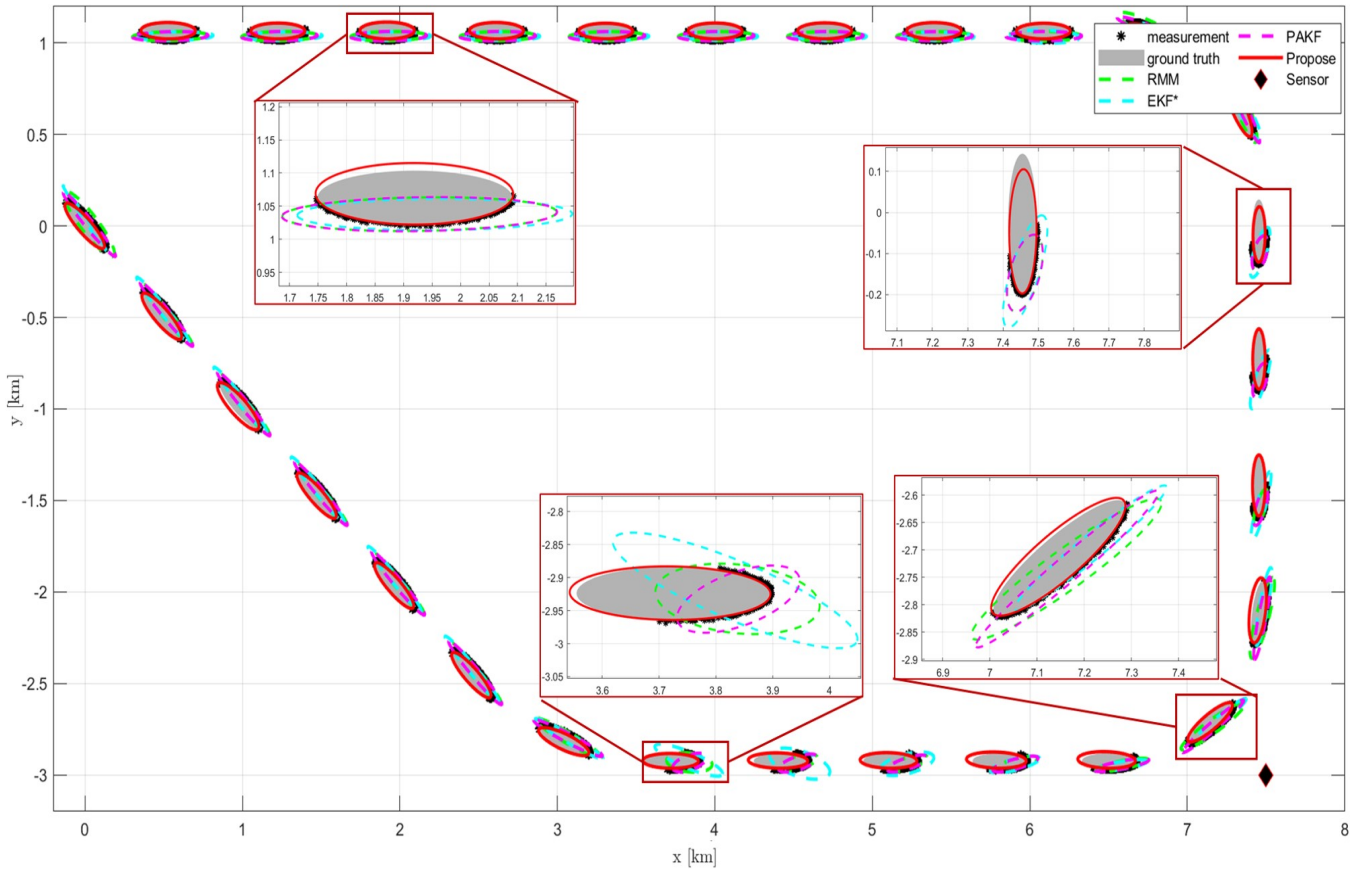


Figure 3 – Simulation data trajectory result

4.1 Evaluation of the Moment Approximations

Initially, the performance of the proposed moment approximation for the shape parameter (16) is evaluated through a comparative analysis with baseline methodologies. To isolate and assess the efficacy of the moment approximation specifically during measurement updates, the evaluation is restricted to a stationary target scenario. The simulation results are illustrated in Fig. 2. Measurements are generated from a uniform distribution spanning an object with dimensions of 8m by 4m. In accordance with the study's focus on dense contour sensing, the number of detections per scan is sampled from a Poisson distribution with a mean (λ) of 25. The process noise covariance matrices for the kinematic and extent states were selected based on a constant-velocity motion assumption for the centroid and a slowly varying shape model for the ellipse parameters. In particular, the extent process noise was chosen to reflect gradual variations in semi-axes and orientation, and its magnitude was tuned to balance responsiveness and estimation stability under measurement uncertainty.
In scenarios where contour measurements are restricted to the sensor-facing boundary, accurately reconstructing the full spatial extent of the target poses a significant challenge. The proposed methodology demonstrates the capability to estimate the complete elliptical morphology even from partial observations by leveraging affine transformations to incorporate geometric priors. In contrast, the PAKF and EKF methods tend to fit the ellipse solely to the instantaneous measurements, thereby neglecting the inherent geometric relationship between the sensor and the target. While the RMM approach employs a Bayesian framework to approximate the measurement distribution, it exhibits substantial estimation bias and fails to achieve acceptable accuracy under these highly constrained sensing conditions.

4.2 Experiments with Simulated Data

The scenario under consideration involves the identification of a particular target object, the extent of which is not known. The true trajectory, object properties, and environmental conditions are similar to those in [6]. However, measurement sources are generated from the object contour in the direction

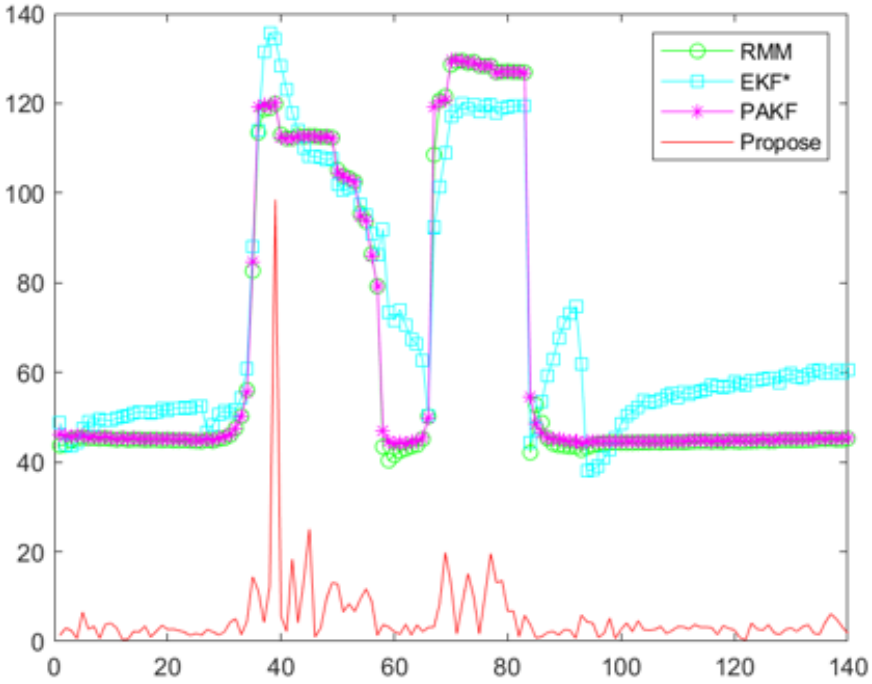


Figure 4 – Extension error by mean square Gaussian Wasserstein distance over MC 100 runs: x-axis is observation step and y-axis is GW mean square error $[m]$.

seen by the sensor located at $[7.5km, -3km]$. The quantity of measurements obtained from a single time scan is derived from a Poisson distribution with a mean of 200. The variances of the measurement noise are $10m^2$ for each dimension. Measurements, trajectory, and estimation results of an example run are depicted in Fig. 3. As demonstrated in Fig. 4, the GW mean square error has been presented over a series of 100 Monte Carlo (MC) runs. It should be noted that conventional methods such as RMM, MEM-EKF*, and PAKF are derived under the assumption of surface-distributed measurements. In contrast, the simulated data in this study are generated from sensor-facing boundary measurements, which introduces a structural model mismatch for these baselines and significantly affects both extent and centroid estimation accuracy. Our method exhibits a comparable overall performance to other approaches in terms of accuracy. However, it should be noted that EKF* and PAKF demonstrate higher errors at the bend part of the trajectory.

Table 1 – Performance Result

	GW error $[m]$	Computation time $[ms]$
RMM	64.84	0.67
EKF*	70.62	3.5
PAKF	65.38	**0.1**
Proposed	**9.15**	0.94

Table I summarizes the comparative performance metrics of the evaluated algorithms. The average extent error, quantified by the Gaussian Wasserstein (GW) distance, was 64.84m for RMM, 70.62m for EKF, and 65.38m for PAKF, whereas the proposed method achieved a significantly lower error of 9.15m. Regarding computational efficiency, the average processing time per scan was 0.67ms for RMM, 3.5ms for EKF, and 0.1ms for PAKF, compared to 0.94ms for the proposed approach. This analysis indicates that while the integration of the affine transformation introduces a marginal computational overhead, the overall latency remains well within the sub-millisecond range, ensuring suitability for real-time applications.

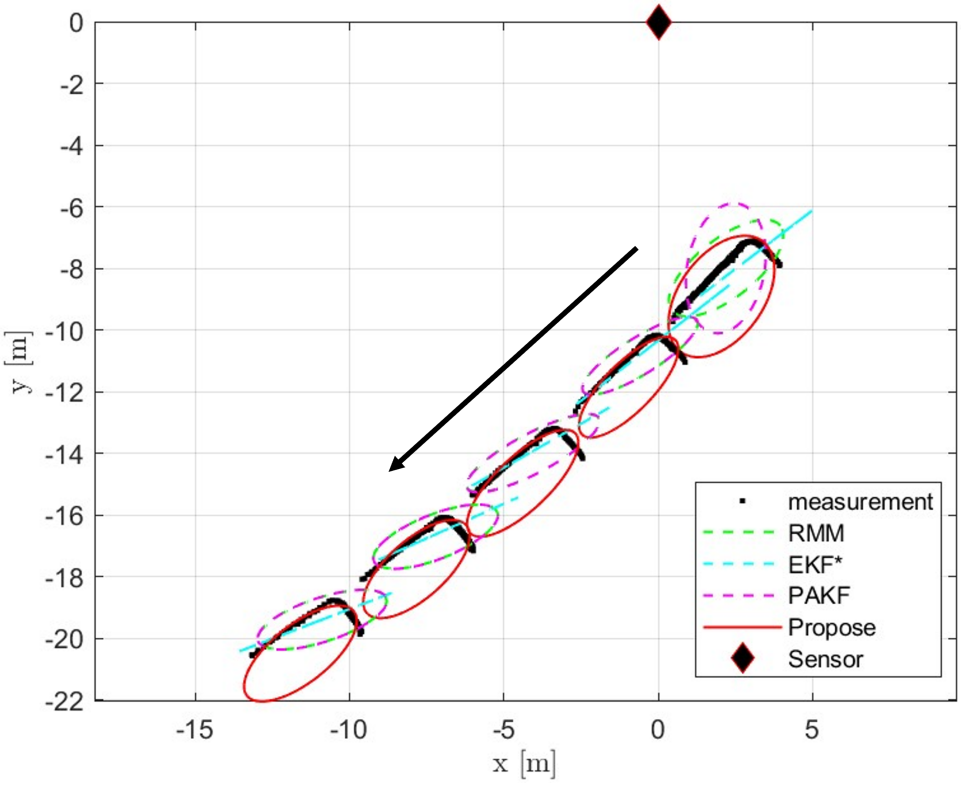


Figure 5 – Real data trajectory result

4.3 Experiments with Real Data

We validate the performance of the proposed algorithm using 2D car tracking point cloud data acquired via a LiDAR sensor. In this scenario, the vehicle traverses diagonally from the upper to the lower region, with only its right and rear facets visible to the LiDAR sensor positioned at the origin $[0,0]$. The measurement density varies according to the sensor-to-target distance, fluctuating between 58 and 235 points per scan. As illustrated in Fig. 5, the proposed method consistently provides accurate extent state estimates, demonstrating robustness even under significantly reduced measurement counts. A clear correlation is observed between the spatial spread of the measurements and the estimated elliptical dimensions, facilitating the gradual convergence of the extent parameters toward their ground-truth values. While the initial trajectory segment exhibited minor deviations due to scan distortion, the estimation accuracy significantly improved as the vehicle progressed, ultimately aligning with the prescribed maneuver.

5. Conclusion

Advancements in sensor technologies have led to a significant increase in the number of measurements obtained from a given target. This study has discovered the problem of elliptical expanded object tracking arising from realistic sensor measurements and solved it by creating algebraic equations. While existing studies may accurately estimate the extent state for small objects based on measurements, but the scaled object size is sufficiently large that measurements do not necessarily determine the size of the object. There are frequent cases where only part of an object is observed without being fully represented. The proposed algorithm was developed under the assumption that the shape model would be best represented by an ellipse. To this end, the algorithm was implemented through a process of ellipse fitting. To assess the efficacy of the proposed approach, a comparative analysis was conducted with other state-of-the-art algorithms on a simulated trajectory. The results of this analysis indicated that the proposed approach has the potential to be a viable candidate for applications that require high processing speed, as evidenced by the simulation results. Furthermore, the tracking algorithm was applied to a real-world standard LiDAR dataset. Through experiments, it has been confirmed that even when only a part of the object is observed, it estimates the extent state of the object very similarly, which the existing algorithm could not accurately estimate.

Acknowledgment

This study has been conducted with the support of the Korea Institute of Industrial Technology as "Development of Image-Based Environment-Adaptive Absolute Navigation Technology for Enhancing Autonomy of Unmanned Vehicles (KITECH UR-26-0073)".

6. Contact Author Email Address

skylih@kitech.re.kr

7. Copyright Statement

The authors confirm that they, and/or their company or organization, hold copyright on all of the original material included in this paper. The authors also confirm that they have obtained permission, from the copyright holder of any third party material included in this paper, to publish it as part of their paper. The authors confirm that they give permission, or have obtained permission from the copyright holder of this paper, for the publication and distribution of this paper as part of the ICAS proceedings or as individual off-prints from the proceedings.

References

[1] Johann Wolfgang Koch. Bayesian approach to extended object and cluster tracking using random matrices. *IEEE Transactions on Aerospace and Electronic Systems*, 44(3):1042–1059, 2008.

[2] KARL GRANSTRöM, MARCUS BAUM, and STEPHAN REUTER. Extended object tracking: Introduction, overview, and applications. *Journal of Advances in Information Fusion*, 12(2), 2017.

[3] Lyudmila Mihaylova, Avishy Y Carmi, François Septier, Amadou Gning, Sze Kim Pang, and Simon Godsill. Overview of bayesian sequential monte carlo methods for group and extended object tracking. *Digital Signal Processing*, 25:1–16, 2014.

[4] Linyuan Zeng, Mingwei Tang, Qianwei Zhang, Xiaoyu Yang, Xu Liu, and Qing Yang. High-resolution true-color imaging based on wavelength-multiplexed far-field spatial-frequency shift imaging. *Optics Express*, 32(25):44987–44998, 2024.

[5] Simon Steuernagel, Kolja Thormann, and Marcus Baum. Improved extended object tracking with efficient particle-based orientation estimation. In *2023 26th International Conference on Information Fusion (FUSION)*, pages 1–8. IEEE, 2023.

[6] Shishan Yang and Marcus Baum. Tracking the orientation and axes lengths of an elliptical extended object. *IEEE Transactions on Signal Processing*, 67(18):4720–4729, 2019.

[7] Karl Granström, Stephan Reuter, Daniel Meissner, and Alexander Scheel. A multiple model phd approach to tracking of cars under an assumed rectangular shape. In *17th International Conference on Information Fusion (FUSION)*, pages 1–8. IEEE, 2014.

[8] Marcus Baum and Uwe D Hanebeck. Extended object tracking with random hypersurface models. *IEEE Transactions on Aerospace and Electronic systems*, 50(1):149–159, 2014.

[9] Barkın Tuncer and Emre Özkan. Random matrix based extended target tracking with orientation: A new model and inference. *IEEE Transactions on Signal Processing*, 69:1910–1923, 2021.

[10] Jian Lan and X Rong Li. Tracking of extended object or target group using random matrix: New model and approach. *IEEE Transactions on Aerospace and Electronic Systems*, 52(6):2973–2989, 2016.

[11] Michael Feldmann, Dietrich Fränken, and Wolfgang Koch. Tracking of extended objects and group targets using random matrices. *IEEE Transactions on Signal Processing*, 59(4):1409–1420, 2010.

[12] Marcus Baum, Florian Faion, and Uwe D Hanebeck. Modeling the target extent with multiplicative noise. In *2012 15th International Conference on Information Fusion*, pages 2406–2412. IEEE, 2012.

[13] Christian Gramsch, Shishan Yang, and Hosam Alqaderi. A batch update using multiplicative noise modelling for extended object tracking. In *2024 27th International Conference on Information Fusion (FUSION)*, pages 1–8. IEEE, 2024.

[14] Felix Govaers. On independent axes estimation for extended target tracking. In *2019 Sensor Data Fusion: Trends, Solutions, Applications (SDF)*, pages 1–6. IEEE, 2019.

[15] Jaya Shradha Fowdur, Marcus Baum, and Frank Heymann. An elliptical principal axes-based model for extended target tracking with marine radar data. In *2021 IEEE 24th International Conference on Information Fusion (FUSION)*, pages 1–8. IEEE, 2021.

[16] Mingkai Li, Jian Lan, and X Rong Li. Tracking of elliptical object with unknown but fixed lengths of axes. *IEEE Transactions on Aerospace and Electronic Systems*, 2023.

[17] Sangjin Lee and James McBride. Extended object tracking via positive and negative information fusion. *IEEE Transactions on Signal Processing*, 67(7):1812–1823, 2019.

[18] Junhao Hua and Chunguang Li. Distributed variational bayesian algorithms over sensor networks. *IEEE Transactions on Signal Processing*, 64(3):783–798, 2015.

[19] Giuseppe Calafiore. Approximation of n-dimensional data using spherical and ellipsoidal primitives. *IEEE Transactions on Systems, Man, and Cybernetics-Part A: Systems and Humans*, 32(2):269–278, 2002.

[20] Zhouchen Lin and Yameng Huang. Fast multidimensional ellipsoid-specific fitting by alternating direction method of multipliers. *IEEE transactions on pattern analysis and machine intelligence*, 38(5):1021–1026, 2015.

[21] Xianghua Ying, Li Yang, and Hongbin Zha. A fast algorithm for multidimensional ellipsoid-specific fitting by minimizing a new defined vector norm of residuals using semidefinite programming. *IEEE transactions on pattern analysis and machine intelligence*, 34(9):1856–1863, 2012.